Charge transfer of keV O⁺ ions with CO and H_2O

B G Lindsay, R Rejoub, D R Sieglaff[1] and R F Stebbings

Department of Physics and Astronomy, and Rice Quantum Institute, Rice University, 6100 Main Street, Houston, TX 77005-1892, USA

Abstract

We report measurements of the absolute differential cross sections (DCSs) for charge-transfer scattering of 0.5–5 keV O⁺ ions by CO and H_2O at scattering angles between 0.04° and 2.9° in the laboratory frame. Estimated total charge-transfer cross sections, derived from these measurements, are compared with previously published data. Cross sections for both $O^+(^4S)$ ground state and $O^+(^2D, {}^2P)$ metastable ions are presented. In contrast to the results of several previous studies the internal energy of the O⁺ ions is found to have little effect on either the angular dependence of the DCSs or on the total cross sections.

1. Introduction

Charge transfer reactions of O⁺ ions play a key role in many environments and they have therefore received considerable attention. However, it has long been recognized that in laboratory studies oxygen ions are typically created in both the ^4S ground state and in long lived metastable states (Stebbings *et al* 1966) and that in collisions with atoms and molecules the behaviour of the O⁺ ions in these various states is generally dissimilar, occasionally markedly so. This has added considerably to the difficulty of conducting experimental investigations of these processes and has limited the scope and accuracy of the published data. The present investigation was motivated, in part, by the need to further our understanding of collisions involving state-selected O⁺ ions at keV energies. Additionally, the work was prompted by the requirement for reliable quantitative data to gauge the effects of CO and H_2O contaminants in our recent O⁺–O resonant charge-transfer study (Lindsay *et al* 2001). Furthermore, there has been renewed interest in the O⁺–H_2O reaction because it is the primary source of water vapour ions in the vicinity of the Space Shuttle (Dressler *et al* 1992) and the present data usefully complement previous low-energy investigations of this reaction.

2. Apparatus and experimental procedure

The apparatus and the experimental method have both been described in detail previously (Lindsay *et al* 1998). The apparatus is shown in figure 1. CO is admitted to a magnetically confined plasma ion source. Ions are extracted from the source through a small aperture,

---

[1] Present address: KLA-Tencor Corporation, MS I-1009, 77 Rio Robles, San Jose, CA 95134, USA.
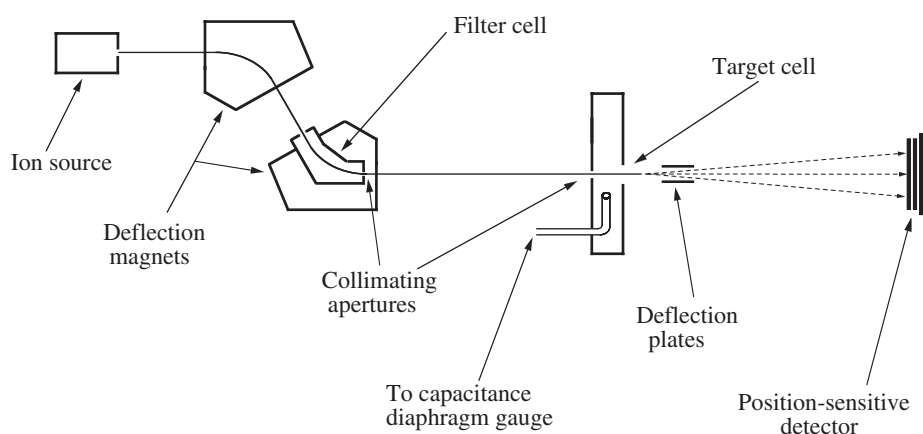
Figure 1. Schematic diagram of the apparatus.

accelerated, and focused to form a beam of the desired energy. Two confocal $60°$ sector magnets are used to select ions of the desired mass-to-charge ratio. Ions passing through a pair of laser drilled apertures form a beam with an angular divergence of approximately $0.03°$. This collimated beam passes through a short target cell and then impacts a position-sensitive detector (PSD), located 26 cm beyond the target cell. The PSD measures the flux of ions passing through the target cell and measures the flux and positions of the impact of the product neutral O atoms. An electric field established between a pair of deflection plates located between the target cell and the PSD is used to deflect the ion beam as required.

In order to measure the differential charge-transfer cross section, either CO or H_2O is admitted to the target cell and the angles of scatter of the neutral O atoms, formed by charge transfer of the primary O^+ ions, are determined from their positions of impact on the PSD. Unscattered primary O^+ ions are normally deflected from the PSD but are allowed to impact the PSD periodically to assess the primary beam flux. These measurements, together with the target number density and target length, are sufficient to determine the differential cross section (DCS). The O^+ beam, as it emerges from the ion source, comprises both $O^+(^4S)$ ground state and $O^+(^2D, {}^2P)$ metastable ions. Cross sections for the different components of the ion beam are obtained by taking advantage of the fact that $O^+(^4S)$ ground-state ions have a much smaller charge-transfer cross section with N_2 than $O^+(^2D, {}^2P)$ metastable ions. In order to measure the ground-state cross section the filter cell is filled with several mTorr of N_2. The emerging O^+ beam then consists essentially of only ground-state ions as practically all of the incident $O^+(^2D, {}^2P)$ ions are converted to neutrals, which because of the apparatus geometry do not enter the target cell (Lindsay *et al* 1998). The $O^+(^2D, {}^2P)$ cross section is then determined by evacuating the filter cell, measuring the effective cross section for the mixed composition beam, determining the fraction of ions in the ground state, and subtracting the contribution these ground-state ions have made to the total scattering signal. The fraction of ions in the ground and excited states is measured using a modified version of the attenuation technique originally developed by Stebbings *et al* (1966). Only two components are identifiable from these attenuation curves, a ground-state component and a metastable excited-state component.

As noted previously (Lindsay *et al* 1999), the attenuation curve technique has certain limitations. For instance, it does not permit the separate contributions of the $O^+(^2D)$ and $O^+(^2P)$ metastable ions to be determined. However, no superior method is currently at hand and the continued use of this technique thus appears warranted. In the context of the present

Table 1. Laboratory frame differential O$^+$–CO charge-transfer cross sections, where E is the projectile energy and the numbers in square brackets represent powers of ten.

Laboratory angle θ (deg)	O$^+$(^{4}S) cross section (10^{-16} cm^2 sr^{-1})			O$^+$(^{2}D, ^{2}P) cross section (10^{-16} cm^2 sr^{-1})		
	$E = 0.5$ keV	$E = 1.5$ keV	$E = 5$ keV	$E = 0.5$ keV	$E = 1.5$ keV	$E = 5$ keV
0.04 ± 0.03	$8.51 \pm 0.21[5]$	$2.40 \pm 0.02[6]$	$2.32 \pm 0.15[6]$	$1.22 \pm 0.03[6]$	$1.67 \pm 0.02[6]$	$2.04 \pm 0.02[6]$
0.09 ± 0.03	$2.92 \pm 0.09[5]$	$3.76 \pm 0.05[5]$	$1.92 \pm 0.03[5]$	$4.69 \pm 0.11[5]$	$3.54 \pm 0.06[5]$	$2.51 \pm 0.04[5]$
0.18 ± 0.03	$7.17 \pm 0.32[4]$	$4.31 \pm 0.12[4]$	$2.74 \pm 0.09[4]$	$1.01 \pm 0.04[5]$	$6.65 \pm 0.17[4]$	$3.90 \pm 0.10[4]$
0.37 ± 0.04	$7.51 \pm 0.76[3]$	$7.96 \pm 0.29[3]$	$4.24 \pm 0.20[3]$	$1.67 \pm 0.09[4]$	$1.14 \pm 0.04[4]$	$5.64 \pm 0.21[3]$
0.71 ± 0.04	$1.66 \pm 0.45[3]$	$1.34 \pm 0.10[3]$	$8.52 \pm 0.75[2]$	$3.75 \pm 0.49[3]$	$2.11 \pm 0.14[3]$	$9.92 \pm 0.70[2]$
1.52 ± 0.17	$2.1 \pm 1.2[2]$	$2.70 \pm 0.19[2]$	$1.33 \pm 0.13[2]$	$9.3 \pm 1.2[2]$	$2.77 \pm 0.21[2]$	$1.60 \pm 0.11[2]$
2.87 ± 0.17	$2.3 \pm 1.3[2]$	$8.9 \pm 1.8[1]$	$6.3 \pm 1.2[1]$	—	$3.7 \pm 1.7[1]$	$2.4 \pm 0.9[1]$

Table 2. Laboratory frame differential O$^+$–H$_2$O charge-transfer cross sections, where E is the projectile energy and the numbers in square brackets represent powers of ten.

Laboratory angle θ (deg)	O$^+$(^{4}S) cross section (10^{-16} cm^2 sr^{-1})			O$^+$(^{2}D, ^{2}P) cross section (10^{-16} cm^2 sr^{-1})		
	$E = 0.5$ keV	$E = 1.5$ keV	$E = 5$ keV	$E = 0.5$ keV	$E = 1.5$ keV	$E = 5$ keV
0.04 ± 0.03	$1.05 \pm 0.05[6]$	$2.15 \pm 0.02[6]$	$2.09 \pm 0.02[6]$	$9.10 \pm 0.38[5]$	$1.26 \pm 0.03[6]$	$1.49 \pm 0.02[6]$
0.09 ± 0.03	$4.47 \pm 0.21[5]$	$3.42 \pm 0.62[5]$	$2.26 \pm 0.04[5]$	$3.60 \pm 0.17[5]$	$2.22 \pm 0.07[5]$	$2.00 \pm 0.04[5]$
0.18 ± 0.03	$8.76 \pm 0.69[4]$	$5.39 \pm 0.18[4]$	$4.21 \pm 0.13[4]$	$6.69 \pm 0.55[4]$	$3.95 \pm 0.20[4]$	$4.38 \pm 0.14[4]$
0.37 ± 0.04	$1.12 \pm 0.18[4]$	$1.09 \pm 0.05[4]$	$7.33 \pm 0.31[3]$	$1.17 \pm 0.14[4]$	$9.01 \pm 0.52[3]$	$7.15 \pm 0.32[3]$
0.71 ± 0.04	$1.3 \pm 1.1[3]$	$3.22 \pm 0.20[3]$	$1.05 \pm 0.10[3]$	$4.40 \pm 0.81[3]$	$2.20 \pm 0.21[3]$	$1.32 \pm 0.10[3]$
1.52 ± 0.17	$5.9 \pm 2.8[2]$	$4.53 \pm 0.33[2]$	$1.34 \pm 0.17[2]$	$8.5 \pm 2.1[2]$	$5.10 \pm 0.32[2]$	$1.64 \pm 0.14[2]$
2.87 ± 0.17	—	$1.3 \pm 0.3[2]$	$4.2 \pm 1.5[1]$	$3.7 \pm 2.3[2]$	$6.6 \pm 2.7[1]$	$4.7 \pm 1.2[1]$

study it has been used solely to determine the fraction of excited-state O$^+$ ions in the beam, rather than the cross sections themselves, and any error resulting from its use in this context should be significantly smaller than the quoted uncertainties in the data presented here.

3. Results and discussion

The DCSs for charge transfer of O$^+$(^{4}S) and O$^+$(^{2}D, ^{2}P) with CO and H$_2$O are shown in figure 2 at energies of 0.5, 1.5, and 5 keV and selected values are tabulated in tables 1 and 2. Besides the statistical uncertainties shown in the graphs there is an additional systematic uncertainty of $\pm 12\%$ in the absolute magnitude of the ground-state DCSs and $\pm 15\%$ in the metastatable-state DCSs. The angular uncertainties arise from the finite primary beam size and the angular resolution used for analysis. All of the cross sections are very forward peaked which is indicative of near-resonant processes and the DCSs for ground-state and metastable-state ions are almost identical, even at the lowest projectile energy.

Due to the limited angular range subtended by the PSD it is only possible to directly measure the scattered O signal out to an angle of approximately 3°. However, from inspection of the DCSs shown in figure 2 it is feasible to infer the extent to which neutrals are scattered at angles sufficiently large to avoid impacting the PSD and by using a simple power-law extrapolation to estimate the true total cross sections. The fraction of scattered neutrals which do not impact the PSD is very small for 5 keV projectiles but increases considerably at the lowest projectile energies studied, and the estimated total cross sections at these energies therefore have correspondingly large uncertainties. The measured integral cross sections (for scattering into angles of 3° or less) and estimated total cross sections (for scattering into all
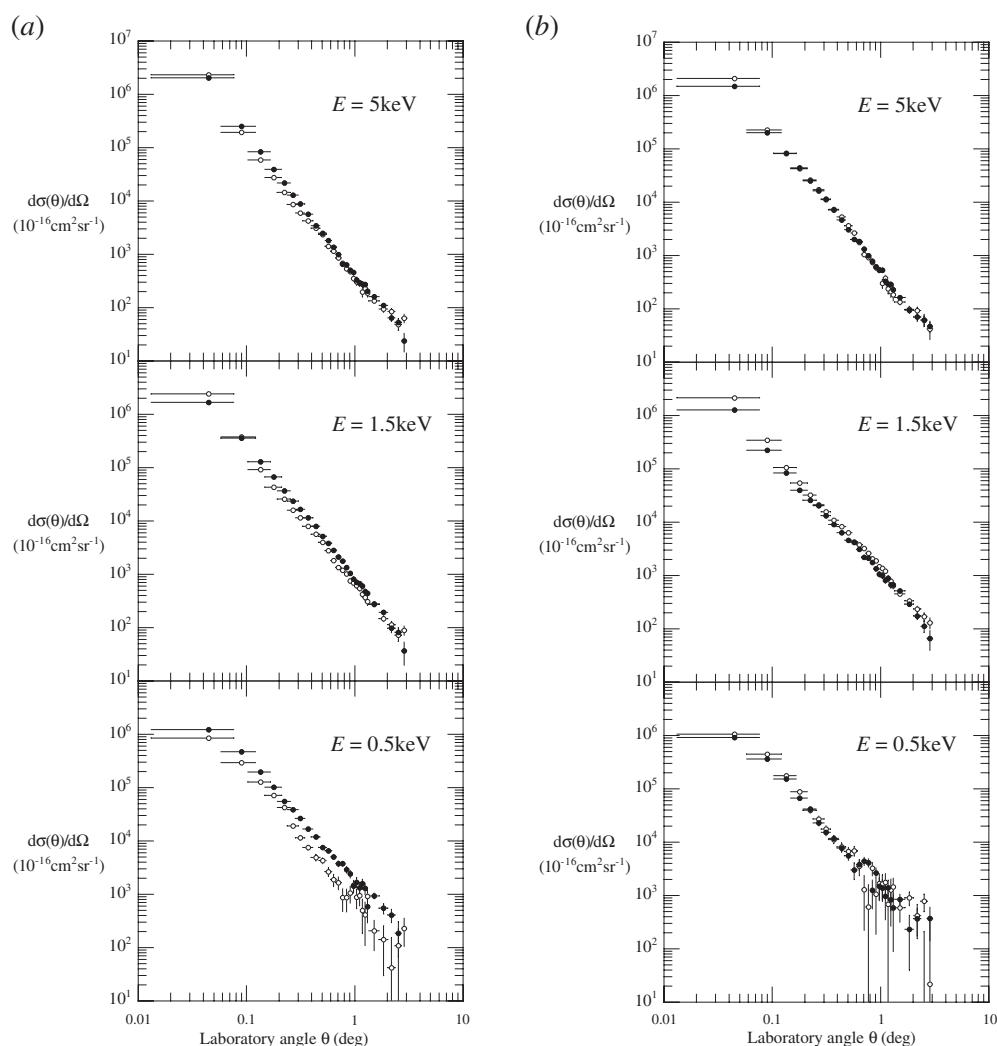
Figure 2. Absolute DCSs for charge-transfer scattering of O^+ ions by (*a*) CO, and (*b*) H_2O at the projectile energies indicated. $O^+(^4S)$ ground-state data are shown as open circles and $O^+(^2D, ^2P)$ metastable data are shown as full circles.

angles) are given in tables 3 and 4. From these tables it is evident that the electronic state of the O^+ projectile has little influence on either the O^+–CO or O^+–H_2O charge-transfer cross section. This is in stark contrast to O^+–N_2, for example, where order of magnitude differences exist between the ground- and excited-state cross sections (Lindsay *et al* 1998). The large differences observed in such cases are often explained qualitatively in terms of the availability of near-resonant reaction pathways, with small energy defects, for one species but not for the other (Stebbings *et al* 1966). O^+–CO and O^+–H_2O provide examples of processes where channels with relatively small energy defects are accessible to both $O^+(^4S)$ and $O^+(^2D, ^2P)$ species and therefore little difference is seen between the cross sections for the ground- and excited-state ions (Moran and Wilcox 1978, Li *et al* 1997). It is of course possible to perform a more detailed quantitative analysis of the present data using the energy defect model, however,
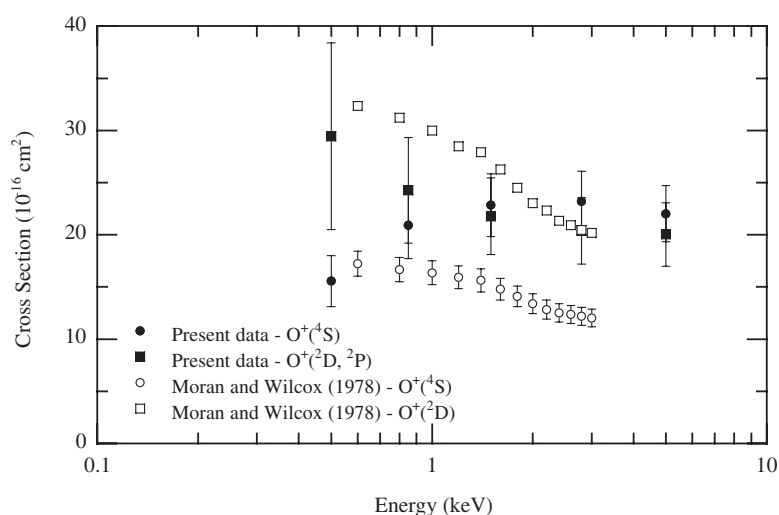
Figure 3. Present O$^+$–CO total charge-transfer cross sections compared to those of Moran and Wilcox (1978).

Table 3. Absolute O$^+$–CO charge-transfer cross sections. The angular range for the integral cross sections is 0–3.0°.

Projectile energy (keV)	Integral cross section (10^{-16} cm^2)		Estimated total cross section (10^{-16} cm^2)	
	O$^+$(^{4}S)	O$^+$(^{2}D, ^{2}P)	O$^+$(^{4}S)	O$^+$(^{2}D, ^{2}P)
0.50	14.2 ± 1.7	23.3 ± 3.5	15.6 ± 2.4	29.4 ± 8.9
0.85	19.1 ± 2.3	21.1 ± 3.2	20.9 ± 3.2	24.2 ± 5.1
1.5	21.7 ± 2.6	20.2 ± 3.0	22.9 ± 3.0	21.8 ± 3.7
2.8	22.4 ± 2.7	19.5 ± 2.9	23.2 ± 2.9	20.4 ± 3.2
5.0	21.6 ± 2.6	19.5 ± 2.9	22.0 ± 2.7	20.0 ± 3.1

Table 4. Absolute O$^+$–H$_2$O charge-transfer cross sections. The angular range for the integral cross sections is 0–3.0°.

Projectile energy (keV)	Integral cross section (10^{-16} cm^2)		Estimated total cross section (10^{-16} cm^2)	
	O$^+$(^{4}S)	O$^+$(^{2}D, ^{2}P)	O$^+$(^{4}S)	O$^+$(^{2}D, ^{2}P)
0.50	21.2 ± 2.5	17.8 ± 2.7	28.8 ± 10.1	24.8 ± 9.7
0.85	22.8 ± 2.7	17.5 ± 2.6	30.6 ± 10.5	25.2 ± 10.3
1.5	23.9 ± 2.9	16.2 ± 2.4	28.7 ± 7.1	19.7 ± 5.8
2.8	23.3 ± 2.8	16.7 ± 2.5	25.0 ± 4.2	18.4 ± 4.1
5.0	22.0 ± 2.6	16.9 ± 2.5	22.6 ± 3.2	17.7 ± 3.3

this would be of marginal value as the relative populations of O$^+$(^{2}D) and O$^+$(^{2}P) ions in this study are unknown.

For CO the only prior data appear to be those of Moran and Wilcox (1978) which are shown for comparison in figure 3. Although their metastable results are reported to pertain to O$^+$(^{2}D) ions alone, both O$^+$(^{2}D) and O$^+$(^{2}P) ions were most likely produced in their ion source (Hamden and Brenton 1989). Furthermore, the uncertainty in their metastable data is at least $\pm 7\%$, and may be greater because of assumptions made with regard to their beam composition
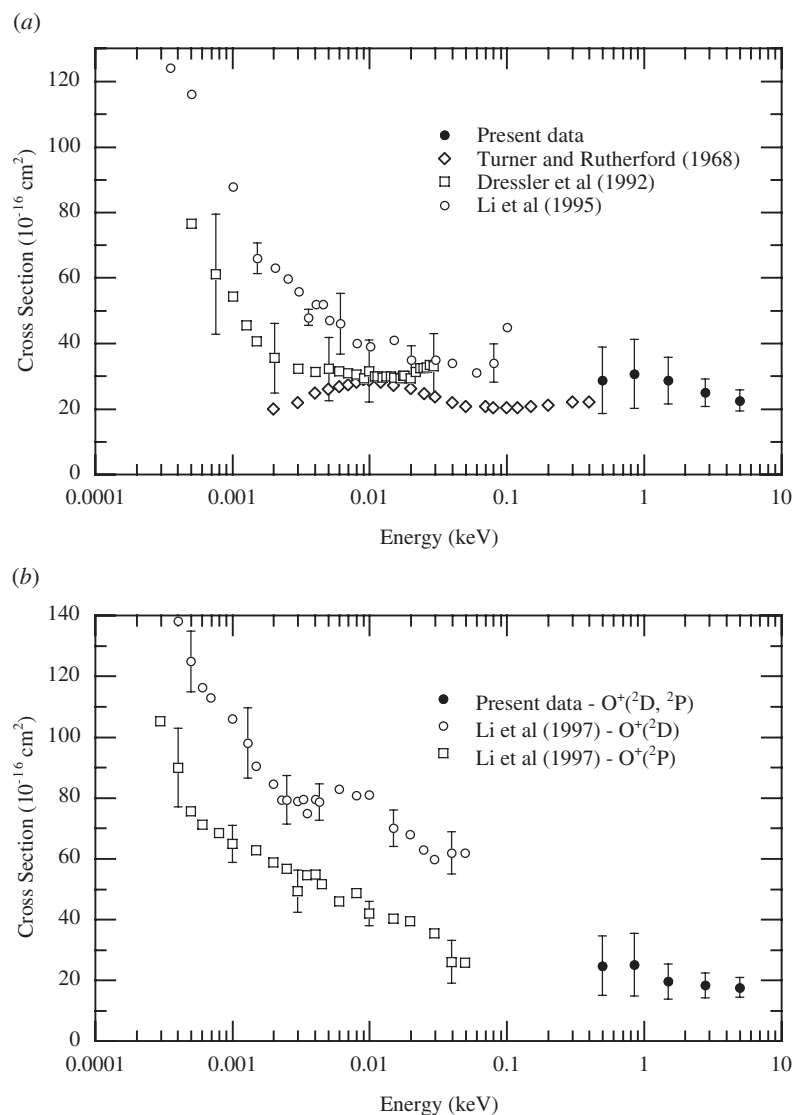
(*a*)

(*b*)

Figure 4. O^+–H_2O total charge-transfer cross sections: (*a*) $O^+(^4S)$–H_2O and (*b*) $O^+(^2D, {}^2P)$–H_2O. Although no overall uncertainty was assigned to the Turner and Rutherford (1968) measurements the major contributor to their uncertainty, the collection efficiency of the system, was known to within approximately $\pm 10\%$.

(Lindsay *et al* 1998). The present ground-state cross section tends to be somewhat higher than that of Moran and Wilcox (1978) while the two metastable cross sections are in fair agreement. Although this situation is not very satisfactory, it should be noted that these discrepancies are actually much smaller than those reported for several other systems (Lindsay *et al* 1998, 1999, Sieglaff *et al* 1999, 2000).

Charge transfer of $O^+(^4S)$ with H_2O has been studied by Turner and Rutherford (1968), Murad and co-workers (Murad and Lai 1986, Heninger *et al* 1989, Dressler *et al* 1990, 1992) and by Li *et al* (1995). Figure 4(*a*) shows that while there are discrepancies between these

various measurements at very low energies they can all be viewed as consistent with the present cross section. The data of Li *et al* (1997) for O$^+$(^{2}D)–H$_2$O and O$^+$(^{2}P)–H$_2$O are shown for comparison with the present O$^+$(^{2}D, ^{2}P)–H$_2$O results in figure 4(*b*). Although this is not a definitive comparison the present measurements are clearly compatible with an extrapolation of the Li *et al* (1997) low-energy data.

4. Conclusion

The absolute DCSs for charge-transfer scattering of 0.5–5 keV O$^+$(^{4}S) and O$^+$(^{2}D, ^{2}P) by CO and H$_2$O at scattering angles between 0.04 and 2.9° in the laboratory frame have been determined. The internal energy of the O$^+$ ions is found to have little effect on either the angular dependence of the DCSs or on the total cross sections. The total cross sections reported here are generally consistent with prior studies although much smaller differences are observed between the ground- and metastable-state O$^+$–CO cross sections.

Acknowledgments

References

Dressler R A, Gardner J A, Salter R H, Wodarczyk F J and Murad E 1990 *J. Chem. Phys.* **92** 1117–25
Dressler R A, Salter R H and Murad E 1992 *Planet. Space Sci.* **40** 1695–704
Hamden M and Brenton A G 1989 *J. Phys. B: At. Mol. Opt. Phys.* **22** 2289–95
Heninger M, Fenistein S, Mauclaire G, Marx R and Murad E 1989 *Geophys. Res. Lett.* **16** 139–41
Li X, Huang Y-L, Flesch G D and Ng C Y 1995 *J. Chem. Phys.* **102** 5100–1
——1997 *J. Chem. Phys.* **106** 928–33
Lindsay B G, Merrill R L, Straub H C, Smith K A and Stebbings R F 1998 *Phys. Rev.* A **57** 331–7
Lindsay B G, Sieglaff D R, Smith K A and Stebbings R F 1999 *J. Phys. B: At. Mol. Opt. Phys.* **32** 4697–704
——2001 *J. Geophys. Res.* at press
Moran T F and Wilcox J B 1978 *J. Chem. Phys.* **69** 1397–405
Murad E and Lai S T F 1986 *Chem. Phys. Lett.* **126** 427–9
Sieglaff D R, Lindsay B G, Merrill R L, Smith K A and Stebbings R F 2000 *J. Geophys. Res.* **105** 10631–5
Sieglaff D R, Lindsay B G, Smith K A and Stebbings R F 1999 *Phys. Rev.* A **59** 3538–43
Stebbings R F, Turner B R and Rutherford J A 1966 *J. Geophys. Res.* **71** 771–84
Turner B R and Rutherford J A 1968 *J. Geophys. Res.* **73** 6751–8